Proc. Natl. Acad. Sci. USA
Vol. 89, pp. 534–538, January 1992
Biochemistry

Crystal structure of an Okazaki fragment at 2-Å resolution

(RNA·DNA hybrid/replication/x-ray crystallography/shock-freezing/A-DNA to B-DNA transition)

MARTIN EGLI, NASSIM USMAN, SHUGUANG ZHANG, AND ALEXANDER RICH

Department of Biology, Massachusetts Institute of Technology, Cambridge, MA 02139

Contributed by Alexander Rich, October 17, 1991

ABSTRACT **In DNA replication, Okazaki fragments are formed as double-stranded intermediates during synthesis of the lagging strand. They are composed of the growing DNA strand primed by RNA and the template strand. The DNA oligonucleotide d(GGGTATACGC) and the chimeric RNA-DNA oligonucleotide r(GCG)d(TATACCC) were combined to form a synthetic Okazaki fragment and its three-dimensional structure was determined by x-ray crystallography. The fragment adopts an overall A-type conformation with 11 residues per turn. Although the base-pair geometry, particularly in the central TATA part, is distorted, there is no evidence for a transition from the A- to the B-type conformation at the junction between RNA·DNA hybrid and DNA duplex. The RNA trimer may, therefore, lock the complete fragment in an A-type conformation.**

DNA replication is a semiconservative process and, in both prokaryotes and eukaryotes, bidirectional growth of both strands starting from a single origin is the most common mechanism (1–3). At the replication fork one of the new DNA strands, the leading strand, grows continuously in the 5′-to-3′ direction. Only one primer at the origin of replication is required by the DNA polymerase to catalyze the addition of nucleotides to the 3′-hydroxyl end of this strand. However, the complementary strand must be replicated in a discontinuous way (4, 5), as DNA polymerases cannot initiate new chains but require a 3′-OH terminus of a primer oligo- or polynucleotide (6). This and the finding that many RNA polymerases are capable of initiating new chains *de novo* (7) led to the discovery that RNA is used for the primers in the synthesis of the lagging strand (8–10). The RNA primers laid down by a primase are then elongated by the DNA polymerase. These short segments of hybrid RNA·DNA plus duplex DNA are referred to as Okazaki fragments.

Double-helical DNA and RNA usually adopt different conformations. In DNA, C2′-*endo* pucker of the deoxyriboses leads to formation of mostly B-type helices. Steric hindrance, due to the presence of the O2′ oxygen in RNA, alters the ribose conformation, resulting in a C3′-*endo* pucker. Several possible interactions of the O2′ oxygen, such as hydrogen bonding to ribose oxygen O1′ of the adjacent residue and water-mediated hydrogen bonding to a phosphate oxygen of the backbone or base atoms may also be important in the formation of an exclusively A-type conformation within double-helical RNA. We have investigated the influence of a short RNA segment on the conformation of double-stranded DNA, as found in Okazaki fragments by x-ray crystallography.*

METHODS

Synthesis, Crystallization, and Data Collection. The sequences of the two strands forming the Okazaki fragment were non-self-complementary to avoid pairing of each of the strands with itself (Fig. 1). The DNA decamer was prepared conventionally by the automated phosphoramidite method on an Applied Biosystems model 380B DNA synthesizer. The large-scale synthesis (10 μmol) of the RNA-DNA chimera was performed according to a modification (N.U. and M.E., unpublished data) of an earlier procedure (11). Both deprotected oligomers were purified by preparative reverse-phase HPLC (column: Rainin Dynamax-300A C_4-silica gel, 12 μm) using 0.1 M triethylammonium acetate (pH 6.5) as the buffer and eluting the oligonucleotides with an acetonitrile gradient. The concentrations of the purified oligonucleotides were determined spectrophotometrically, taking into account the various extinction coefficients of the mononucleotides. The final solution concentrations of both the DNA and the chimeric RNA-DNA strands were adjusted to 5 mM and used for crystal growth.

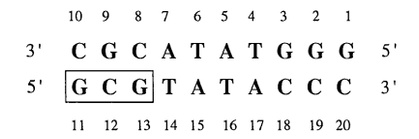

FIG. 1. Sequence of the Okazaki fragment (RNA residues boxed). Note the lack of twofold rotational symmetry.

The two strands were annealed by incubating a 1:1 molar mixture of DNA and chimeric RNA-DNA solutions for 1 h at 90°C and then cooling the mixture to room temperature in a water bath overnight. Crystals were grown at 18°C in sitting drops using the vapor diffusion method. The crystallization mother liquor initially contained 1.5 mM Okazaki fragment (DNA strand plus chimeric RNA-DNA strand), 30 mM sodium cacodylate buffer (pH 7), 7.8 mM magnesium chloride, and 75 mM spermine tetrachloride. The sitting drops were equilibrated against a reservoir of 20 ml of 40% (vol/vol) 2-methyl-2,4-pentanediol. Crystals began to appear within 1 month as distorted bipyramids and grew to a typical size of 0.3 × 0.3 × 0.5 mm. Analysis of the crystals using gel electrophoresis showed the presence of both strands. Diffraction quality crystals were only obtained at pH values of 7 or higher and the spermine tetrachloride concentration in the set-up dips was typically 50 times higher than the concentration of the two oligonucleotide strands. A reduction of either pH or spermine concentration resulted in soft crystals of lower quality or formation of oil droplets. Crystals could only be grown with 1:1 molar mixtures of DNA strand and chimeric RNA-DNA strand. No crystals were obtained from solutions containing either the DNA strand or the chimeric RNA-DNA strand by itself under otherwise identical conditions as in the crystallizations of 1:1 molar mixtures.

Initial diffraction data were collected at room temperature to a resolution of 2.5 Å (space group, $P2_12_12_1$, cell constants,

The publication costs of this article were defrayed in part by page charge payment. This article must therefore be hereby marked "*advertisement*" in accordance with 18 U.S.C. §1734 solely to indicate this fact.

*The atomic coordinates have been deposited in the Protein Data Bank, Chemistry Department, Brookhaven National Laboratory, Upton, NY 11973 (reference 10 FX).

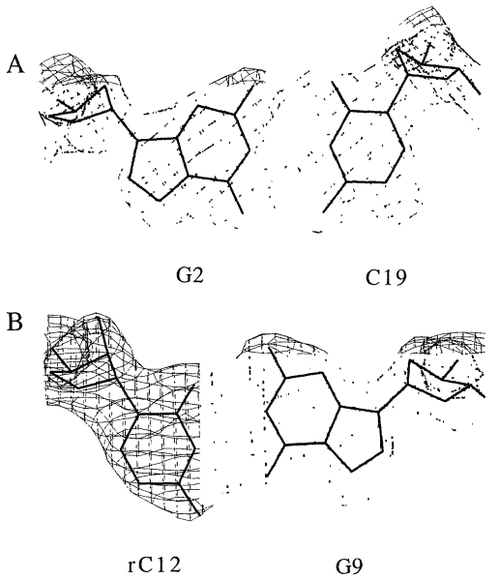

FIG. 2. Final Fourier electron sum density ($2F_{obs} - F_{calc}$) around base pairs G(2)·C(19) (*A*) and G(9)·rC(12) (*B*). The maps were generated using 1826 reflections with $F_{obs} > 2\sigma(F_{obs})$ between 10- and 2-Å resolution. The pseudo-twofold symmetry of the Okazaki fragment could lead to two distinct orientations in the crystal lattice. Equal occupation of these orientations would result in superposition of guanine and cytosine bases in the above base pairs; however, the maps show the predominance of one orientation.

a = 24.82 Å, b = 45.22 Å, and c = 47.92 Å). To reduce the rate of crystal decay, a second data set with slightly improved resolution was measured at 10°C. Slowly cooling the crystal in a capillary to lower temperatures resulted in broadening and sometimes splitting of the diffraction peaks. A third data set was then obtained by shock-freezing a crystal at −110°C in a cold N_2 gas stream (12). Data were collected on a Rigaku AFC5R four-circle diffractometer equipped with a rotating copper anode and graphite monochromator ($\lambda_{CuK\alpha}$ = 1.5406 Å). The cell constants were a = 24.03 Å, b = 43.67 Å, and c = 48.95 Å. A total of 3858 reflections were measured by the ω scan method with a scan speed of 4°/min, and no decay of the crystal was observed. Data were corrected for Lorentz and polarization effects and a semiempirical absorption correction based on Ψ scans for three reflections with χ values greater than 85° was applied (13). This shock-freezing procedure improved the resolution to 2 Å with 1860 unique reflections observed above the $2\sigma(F_{obs})$ level, where F_{obs} is the observed structure factor and σ is its standard deviation.

Structure Solution and Refinement. The structure was solved with the second data set using the molecular replacement method with the program ULTIMA (14) and an A-type conformation search model (15). The correct solution resulted in a residual error (R) factor of 47% including data between 25 and 3 Å. This model was then refined using the low-temperature data with the Konnert–Hendrickson least-squares procedure (16), as modified for nucleic acids (17). The resolution was extended from 3 to 2 Å in several steps [1826 reflections with $F_{obs} > 2\sigma(F_{obs})$ between 10- and 2-Å resolution]. At this point the orientation of the duplex with respect to its pseudo-twofold rotation axis was still ambiguous (see Fig. 1). Both orientations were, therefore, refined without the O2′ oxygens for the same number of cycles using 2-Å data. One of the two orientations resulted in a 3% lower R-factor than the other (25% and 28%). Fourier electron sum ($2F_{obs} - F_{calc}$) and difference ($F_{obs} - F_{calc}$) density maps (where F_{calc} is the calculated structure factor) were calculated and displayed on an Evans and Sutherland (Salt Lake City) PS390 graphics terminal using the program FRODO (18). For

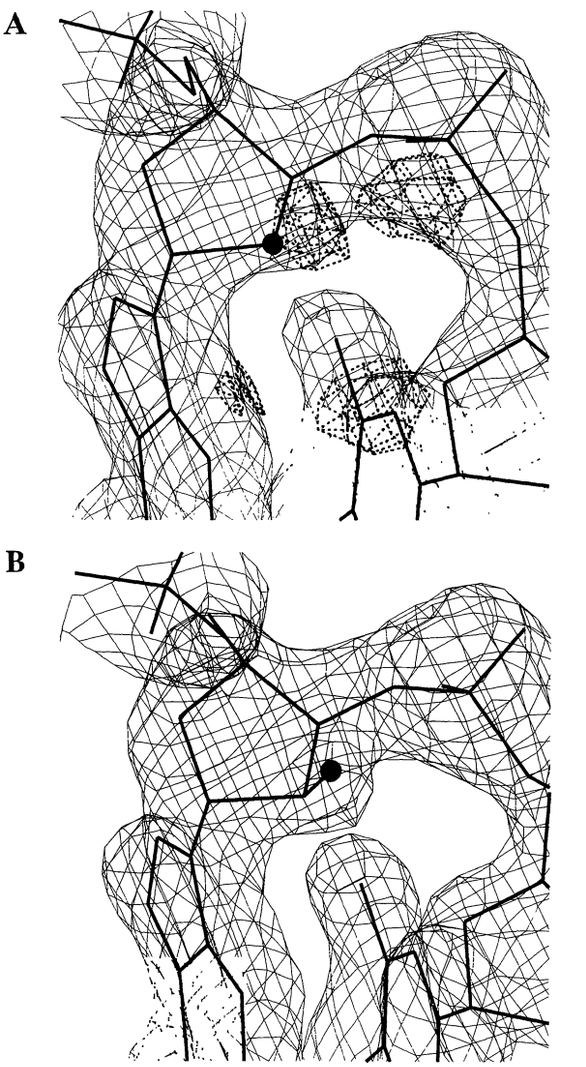

FIG. 3. (*A*) Sum and difference ($F_{obs} - F_{calc}$) density around the ribose of residue rG(13), before addition of the O2′ oxygen (R-factor, 19%; 2-Å data). The C2′ carbon is highlighted with a large dot. The superimposed sum (thin lines) and difference densities (dashed lines) around C2′ indicate the missing O2′ oxygen [residue rC(12) is similar]. (*B*) Identical to view in *A*, showing the sum density after the final refinement steps (no difference density is present at the same display level as in *A*). The position of the O2′ oxygen is highlighted with a large dot. The densities around the O2′ oxygens of residues rC(12) (visible in Fig. 2*B* at the very left) and rG(11) are resolved similarly.

the model that showed the lower R-factor, the sum density around the two critical base pairs was well resolved and all atoms were in density (Fig. 2). In contrast several base atoms were out of density with the other model. Refinement was continued with the preferred structure, solvent molecules were included, and their positions were refined without releasing the constraints. At an R-factor of 19%, maps showed superimposed sum and difference density at the positions of the expected O2′ oxygens of residues rC(12) and rG(13) (Fig. 3*A*), but no difference density around the C2′ positions of residues G(1), G(2), and G(3). The maps around the ribose of residue rG(11) suggested an altered position of the entire ribose. The O2′ oxygens of residues rC(12) and rG(13) were included in the refinement, the ribose of residue rG(11) was rebuilt and its O2′ oxygen was included after additional refinement. The constraints were gradually released and, at an R-factor of 15.6% for 1826 reflections,

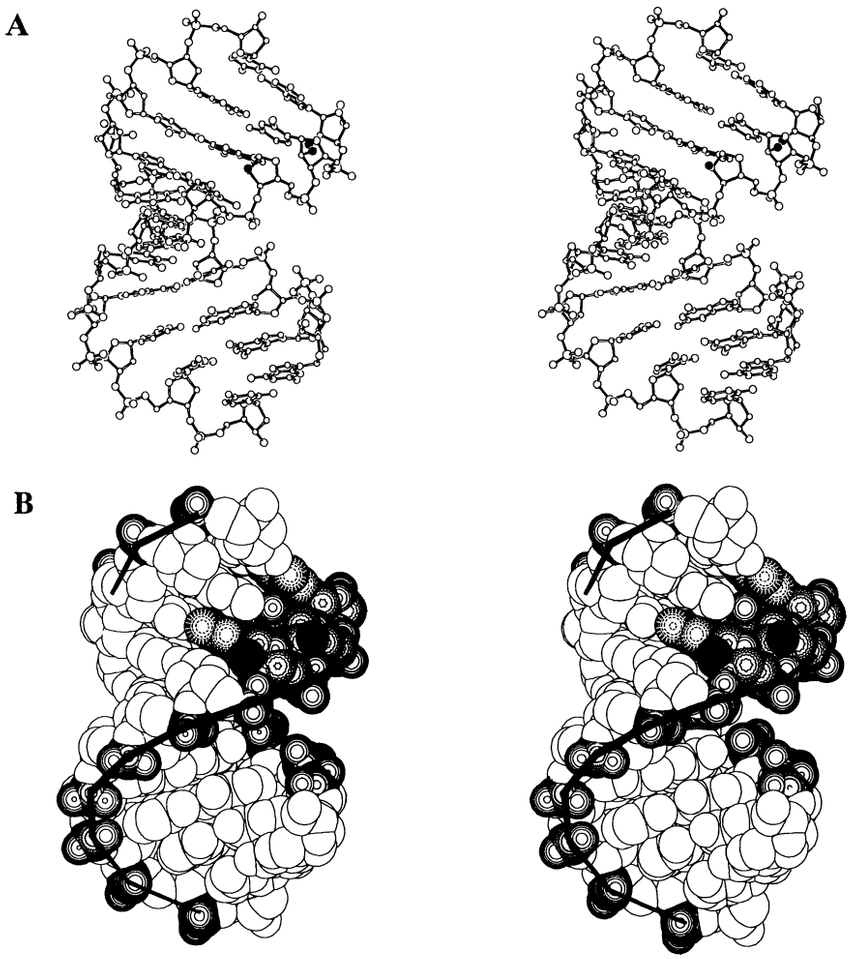

FIG. 4. (*A*) Stereo skeletal drawing of the Okazaki fragment (minor groove on the left and major groove on the right). The RNA primer (to the upper right) is drawn with solid bonds and the DNA is drawn with open bonds. The DNA strand dG(1) to dC(10) runs from the upper right to the lower left; the chimeric RNA-DNA strand rG(11) to dC(20) runs from the upper right to the lower left. Atom types are coded according to size with P > O > N > C and O2′ oxygens are solid. (*B*) Stereo van der Waals representation of the Okazaki fragment (view identical to *A*). Darker patterns highlight RNA atoms (carbons, wavy circles; oxygens, concentric circles; nitrogens, dashed circles; O2′ oxygens, solid black) and phosphate groups are traced with solid lines to emphasize the backbones. Note that only the O2′ oxygens of residues rC(12) and rG(13) are lying at the surface of the minor groove and that the O2′ oxygen of residue rG(11) is located in the major groove and, therefore, is hidden.

refinement was stopped. All atoms were in sum density, and the sum densities around base pairs G(2)·C(19) and G(9)·rC(12) (Fig. 2) and around the O2′ oxygens (Fig. 3*B*) were well resolved. The final asymmetric unit contained the Okazaki fragment, one spermine molecule, and 93 water molecules. The rms deviations from ideality for bond lengths were 0.016 Å and for bond angles they were smaller than 1°.

RESULTS AND DISCUSSION

The Okazaki fragment adopts an overall A-type conformation with 11 residues per turn and shows similarities to the fiber structure of A-RNA (19). The averaged backbone torsion angles† (standard deviations in degrees are the first numbers in parentheses; the averaged values in degrees found in the A-RNA fiber structure by Arnott *et al.* (19) are the second numbers in parentheses) are: $\alpha = -62°$ (38, −60), $\beta = 167°$ (17, 175), $\gamma = 62°$ (51, 49), $\delta = 85°$ (20, 83), $\varepsilon = -158°$ (22, −147), and $\zeta = -70°$ (22, −78). The backbone conformations of the two strands are quite similar and the rms deviation for backbone atoms between the two strands is 0.56 Å. The average distance between adjacent phosphorous atoms is 5.9 Å; the major groove is 5.4 Å wide and about three times as deep as the minor groove, which is 10.2 Å wide (Fig. 4). The average rise per step is 2.5 Å (SD = 0.3 Å) and the average twist is 33° (SD = 3°).

All base pairs display large propeller twists, the average value being −14° with a maximum value of −21° in base pairs T(6)·A(15) and A(7)·T(14) and a minimum value of −5° in the terminal base pair G(1)·C(20). The base pairs C(8)·rG(13) and A(7)·T(14) show much higher buckle than all the other base pairs (−17° and −13°, respectively). It is important that these two base pairs lie at the junction between the RNA·DNA hybrid and the DNA duplex (Figs. 1 and 4*A*). Some base pairs show a considerable amount of sliding of the two bases along each other in a direction normal to Watson–Crick hydrogen bonds (shear). Of the three G·C base pairs formed by the RNA trimer and the bases of the opposite DNA residues, C(8), G(9), and C(10), the two terminal base pairs display considerable shearing. In the terminal base pair C(10)·rG(11), the distance between N3 of residue C(10) (acceptor) and N1 of residue rG(11) (donor) is 2.87 Å. Because of the shear, this hydrogen-bonding distance is just slightly shorter than the distance between N2 of residue rG(11) and the same N3 acceptor of C(10) (2.98 Å). Thus N2 of residue rG(11) is lying between the two donors O2 and N3 of C(10) and may form a bifurcated or three-center hydrogen bond. For base pair G(9)·rC(12), the amount of shearing is similar, but N1 of residue G(9) (donor) is now lying between acceptors N3 and O2 of residue rC(12) (the distances are 2.82 Å and 2.77 Å, respectively) and may also form a bifurcated hydrogen bond. The distance between O6 of residue G(9) and N4 of residue rC(12) is 2.76 Å and the distance between N2 of residue G(9) and O2 of residue rC(12) is 3.02 Å (this base pair is depicted in Fig. 2*B*). Whereas the two terminal base pairs of the RNA·DNA duplex are sheared by about 1 Å, the three G·C base pairs in the DNA duplex at the opposite end show no shearing. However, the base pairs in the central TATA part show deviations from standard Watson–Crick hydrogen bonding. Sliding of the bases in their plane along the normal

†Torsion angles are defined as O3′–P–α–O5′–β–C5′–γ–C4′–δ–C3′–ε–O3′–ζ–P–O5′.

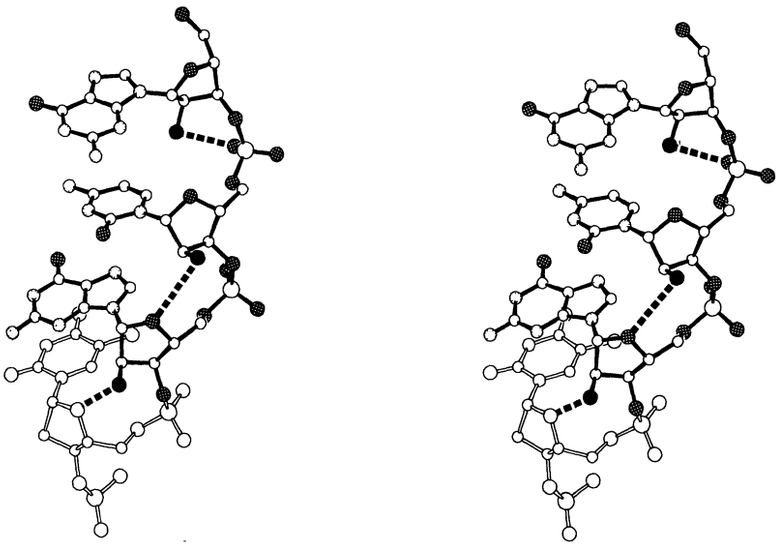

FIG. 5. Stereo drawing of the RNA primer [solid bonds, residue rG(11) at the top]. DNA residue T(14) (open bonds) has been included for orientation. Nitrogen atoms are stippled in grey, oxygen atoms are stippled in black, O2′ oxygens are solid, and hydrogen bonds are dashed.

to the hydrogen-bonding direction results in an elongation of the hydrogen-bond distance between N6 of adenines and O4 of thymines in the A·T base pairs. The average donor–acceptor distance for the N1 (adenine)–N3(H) (thymine) hydrogen bonds is 2.84 Å and for N6(H) (adenine)–O4 (thymine) hydrogen bonds, the average distance is 3.02 Å. The N(H)–O distances for the three A·T base pairs at the junction are 3.04 Å, 3.00 Å, and 3.17 Å. For the A·T base pair adjacent to the three G·C base pairs formed by the DNA duplex, the distance is 2.87 Å. Similar discrepancies for the hydrogen-bond geometry in the TATA section were observed in the crystal structure of the RNA·DNA hybrid with an RNA trimer in each strand (15).

With two exceptions, the riboses and deoxyriboses show C3′-*endo* puckering as expected with the A-type conformation. These two exceptions are the deoxyribose of the terminal residue G(1) and the ribose of the terminal residue rG(11) in the RNA trimer. The deoxyribose of G(1) shows C2′-*exo* puckering (pseudo rotation angle, −35°) and the ribose of rG(11) shows C3′-*exo* puckering (pseudo rotation angle, 190°). The slightly higher energy of the C3′-*exo* pucker in the latter case might be compensated by the formation of a hydrogen bond between O2′ of rG(11) and the phosphate oxygen O1P of the adjacent residue (distance, 2.84 Å; Figs. 4*A* and 5). The formation of this hydrogen bond leads to a rotation of the ribose around an axis formed by C1′ and C3′ and an altered backbone conformation. The torsion angles for this residue are $\gamma = 142°$, $\delta = 161°$, $\varepsilon = -172°$, and $\zeta = -118°$ and differ considerably from the average values given above. This particular conformation puts the O2′ of this residue in the major groove. It is therefore not visible in the space-filling model shown in Fig. 4*B*. Although this interaction of an O2′ with a phosphate oxygen may be related to the larger conformational freedom of the terminal residue, it shows an alternative stabilization of the A-type conformation in RNA. The O2′ oxygen now lying in the deep and narrow major groove is no longer accessible to interacting molecules. Besides the contact to the phosphate oxygen, O2′ of the terminal residue rG(11) forms a hydrogen bond to a water molecule (3.19 Å). The other two O2′ oxygens are located at the surface of the minor groove and are thus accessible to molecules interacting with the A-RNA by the shallow and wide minor groove. The O2′ oxygen of residue rC(12) lies 3.42 Å from oxygen O1′ of the adjacent residue rG(13) (Fig. 5). Oxygen O2′ of residue rG(13) lies 3.43 Å from oxygen O1′ of the adjacent residue T(14) and forms an additional contact to a water molecule (3.36 Å). It should be noted that none of the O2′ oxygens is involved in direct contacts to neighboring molecules or in lattice contacts mediated by water molecules. The spermine molecule lies across the minor groove, forming contacts to three neighboring duplexes through hydrogen bonds and van der Waals interactions.

A number of suggestions have been made to explain the role of the O2′ oxygens in the stabilization of an A-type conformation with double-stranded RNA (for summary, see ref. 20). One possibility is weak hydrogen bonds between the O2′ oxygens and the O1′ oxygens of adjacent riboses. In such an arrangement, the O2′ oxygens are located at the rim of the minor groove, running parallel to the phosphate groups of the backbone. The above distances between the O2′ oxygens and the adjacent O1′ oxygens (3.42 Å and 3.43 Å) are rather long. These hydrogen bonds are weak and cannot be the crucial factor in the stabilization of the A-type conformation in the present case. For the interaction between O2′ of residue rC(12) and O1′ of residue rG(13), the angle at the donor atom (C2′–O2′–O1′) is 72°. For the interaction between O2′ of residue rG(13) and O1′ of residue T(14), the angle at the donor atom is 71°. These geometries are another indication that hydrogen-bond interactions of the above type are weak and that additional factors must contribute to the C3′-*endo* stabilization not just in the RNA primer but essentially in the complete Okazaki fragment. One of these factors could be steric hindrance caused by the O2′ oxygen, which would prohibit other sugar pucker modes. Another reason for stabilization of the A-type conformation might be packing forces.

There are extensive lattice contacts between duplexes in the structure of the Okazaki fragment. Each duplex forms direct contacts to four neighbor duplexes. The terminal base pairs of each duplex are reaching into the minor grooves of two adjacent duplexes, where they are stacked on deoxyriboses. Its own deoxyriboses are stacked on the terminal base pairs of two other duplexes. The terminal base pair G(1)·C(20) is stacked on the deoxyriboses of residues A(7) and C(8) of another duplex. In addition, oxygen O3′ of residue C(20) is located at 3.41 Å from N2 of residue rG(13) from the same neighbor. The other terminal base pair C(10)·rG(11) forms stacking interactions with the deoxyribose of residue C(19) of a second neighbor. The shortest contact is between N1 of rG(11) and O1′ of the deoxyribose (3.03 Å). The terminal oxygen O3′ of residue C(10) forms a hydrogen bond to N2 of G(2), located in the minor groove of the same neighbor (2.70 Å).

It is known that the B-type geometry is preferred by duplex DNA with alternating purine-pyrimidine sequences (21). Nevertheless, there is a slight possibility that the A-type

conformation is intrinsically adopted by an all-DNA duplex with the above Okazaki fragment sequence in the crystalline state. To address this question, crystals of the all-DNA self-complementary sequence d(GCGTATACGC) were grown. The crystals show entirely different morphology from the above Okazaki fragment crystals and preliminary crystallographic investigations reveal a hexagonal packing with cell parameters $a = b = 27.3$ Å and $c = 132.2$ Å. Although the crystals diffract poorly, the different lattice and a strong 10th layer line in diffraction pictures (characteristic for B-DNA) are a strong indication that the conformations of the hybrid duplex and the all-DNA duplex with a very similar sequence are different. It appears therefore that the small single-stranded RNA primer is driving the longer double-stranded DNA fragment, normally adopting the B-type conformation, into an A-type conformation. Although the hybrid segment and the TATA section of the double-stranded DNA portion show significant distortions in their base-pair geometries, there is no evidence for a transition from the A- to the B-type conformation in this Okazaki fragment.

It is unclear how long the double-stranded DNA stretch needs to be to induce a conformational transition with a duplex containing an RNA-DNA strand. Earlier NMR investigations with a $dG_n{\cdot}rC_{11}$-dC_{16} Okazaki-type hybrid had suggested a coexistence of two helical conformations in the fragment (22) and models of A–B junctions comprising 3 base pairs were proposed (23). More recently, NMR studies on short $[DNA\text{-}RNA\text{-}DNA]_2$ duplex chimeras showed a structural perturbation at the junction site that is spread over at least 2 base pairs (24). Such junctions occurring over a few base pairs would provide evidence against the propagation of secondary structure along the DNA duplex. However, the uniform A-type geometry of the present structure suggests a more important role of the RNA part in RNA·DNA hybrids than previously assumed. The distortions found in base pairs in the central TATA sequence could be sequence dependent and are perhaps not a characteristic of the hybrid. Distortions in this sequence were also found in the duplex formed by a self-complementary decamer, containing three RNA residues (15). That structure also has an A-type conformation. The structure of an all-RNA duplex with the same sequence might provide an answer as to whether the above distortions are sequence-dependent. Surprisingly, self-complementary decamer hybrids with just one RNA residue per strand adopt a regular A-type conformation as well (M.E. and N.U., unpublished data). Obviously, a much longer stretch of DNA is necessary to induce a change from the A- to the B-type conformation. Therefore, RNA not only may serve as the primer in DNA replication but also, by inducing and locking an A conformation may play a role in longer-range interactions.

We thank Prof. Olga Kennard for helpful comments and suggestions with the manuscript, Dr. Daniel Bancroft for help with the low-temperature measurement, and the members of the Rich group for discussions. This research was supported by grants from the National Institutes of Health, the American Cancer Society, the National Science Foundation, the Office of Naval Research, and the National Aeronautics and Space Administration. M.E. acknowledges fellowship support from the Geigy-Jubiläums-Stiftung, N.U. was funded by a National Institutes of Health Fogarty International Research Fellowship, and S.Z. is a Fellow of the American Cancer Society.

1. Meselson, M. & Stahl, F. W. (1958) *Proc. Natl. Acad. Sci. USA* **44,** 671–682.
2. Huberman, J. A. & Riggs, A. D. (1968) *J. Mol. Biol.* **32,** 327–341.
3. Fareed, G. C., Garon, C. F. & Salzman, N. P. (1972) *J. Virol.* **10,** 484–491.
4. Okazaki, R., Okazaki, T., Sakabe, K. & Sugimoto, K. (1967) *Jpn. J. Med. Sci. Biol.* **20,** 255–260.
5. Okazaki, R., Okazaki, T., Sakabe, K., Sugimoto, K. & Sugino, A. (1968) *Proc. Natl. Acad. Sci. USA* **59,** 598–605.
6. Kornberg, A. (1974) *DNA Replication* (Freeman, San Francisco), p. 367.
7. Maitra, U. & Hurwitz, J. (1965) *Proc. Natl. Acad. Sci. USA* **54,** 815–822.
8. Brutlag, D., Schekman, R. & Kornberg, A. (1971) *Proc. Natl. Acad. Sci. USA* **68,** 2826–2829.
9. Sugino, A., Hirose, S. & Okazaki, R. (1972) *Proc. Natl. Acad. Sci. USA* **69,** 1863–1867.
10. Okazaki, R., Sugino, A., Hirose, S., Okazaki, T., Imae, Y., Kainuma-Kuroda, R., Ogawa, T., Arisawa, M. & Kurosawa, Y. (1973) in *DNA Synthesis in Vitro*, eds. Wells, R. D. & Inman, R. B. (University Park Press, Baltimore), pp. 83–106.
11. Scaringe, S. A., Francklyn, C. & Usman, N. (1990) *Nucleic Acids Res.* **18,** 5433–5441.
12. Hope, H. (1988) *Acta Crystallogr. Sect. B* **44,** 22–26.
13. North, A. C. T., Phillips, D. & Matthews, F. S. (1968) *Acta Crystallogr. Sect. A* **24,** 351–359.
14. Rabinovich, D. & Shakked, Z. (1984) *Acta Crystallogr. Sect. A* **40,** 195–200.
15. Wang, A. H.-J., Fujii, S., van Boom, J. H., van der Marel, G. A., van Boeckel, S. A. A. & Rich, A. (1980) *Nature (London)* **299,** 601–604.
16. Hendrickson, W. A. & Konnert, J. H. (1981) in *Biomolecular Structure, Conformation, Function and Evolution*, ed. Srinivasan, R. (Pergamon, Oxford), pp. 43–57.
17. Quigley, G. J., Teeter, M. M. & Rich, A. (1978) *Proc. Natl. Acad. Sci. USA* **75,** 64–68.
18. Jones, T. A. (1978) *J. Appl. Crystallogr.* **11,** 268–272.
19. Arnott, S., Smith, P. J. C. & Chandrasekaran, R. (1976) in *CRC Handbook of Biochemistry and Molecular Biology,* ed. Fasman, G. D. (CRC, Cleveland), Vol. 2, 3rd Ed., pp. 411–422.
20. Saenger, W. (1984) *Principles of Nucleic Acid Structure* (Springer, New York), 1st Ed., pp. 64–68.
21. Arnott, S., Chandrasekaran, R. & Selsing, E. (1975) in *Structure and Conformation of Nucleic Acids and Protein-Nucleic Acid Interactions*, eds. Sundaralingam, M. & Rao, S. T. (University Park Press, Baltimore), pp. 577–596.
22. Selsing, E., Wells, R. D., Early, T. A. & Kearns, D. R. (1978) *Nature (London)* **275,** 249–250.
23. Selsing, E., Wells, R. D., Alden, C. J. & Arnott, S. (1979) *J. Biol. Chem.* **254,** 5417–5422.
24. Chou, S.-H., Flynn, P., Wang, A. & Reid, B. (1991) *Biochemistry* **30,** 5248–5257.